

Comparing Two Engines of 425 kWe with the same Cogeneration Configuration through a Computational Simulation Methodology

Denilson Boschiero do Espirito Santo
Mechanical Engineering Faculty, Energy Department
State University of Campinas, SP, Brazil
denilson@fem.unicamp.br

Abstract

Cogeneration systems have proved to be a good choice for decentralized power generation in sites of coincident electrical and thermal loads. However, site electrical and thermal demands can vary substantially with the hour of the day, which makes cogeneration systems achieve a high energy utilization factor (EUF) at hours of high coincident demands, and a low EUF at hours of small coincident demands. In designing such a system, energy supplied by different prime movers should be compared with energy demands, in order to choose the best option. Thermal systems simulation is a useful design tool which helps assess the economical feasibility of different possible cogeneration systems. In this paper, a computational hourly profile simulation methodology that combines curve fittings from literature and manufacturers' data with mathematical representations of physical phenomena is used to predict the performance of one given cogeneration configuration with two different engines, one naturally aspirated and the other turbocharged.

Keywords: Thermal system integration, internal combustion engine, absorption chiller, heat recovery steam generator, computer simulation, software, iterative procedures

1. Introduction

Environmental impacts, scarce or limited natural resources, and a competitive electrical market are some factors that make it important to design cogeneration systems with a high energy utilization factor. The assessment of cogeneration systems involves several variables. Energy balances, load profile calculation and measurement, equipment performance, operational strategies, legislation, operational costs, investment costs, environmental aspects are some of the fields that must be dealt with.

Computational evaluation can reveal important information on the match of the loads to the system under analysis. The design of cogeneration systems may lead to systems that do not meet all energy demands of the site. Therefore, auxiliary equipment must meet particular loads, complementary equipment must meet peak loads, and electricity can be sold and/or be bought from the grid. Legal aspects and fuel and electricity costs can also have an influence in the size of the cogeneration system, leading to design of systems that either produce

excess electricity or produce just the baseline electricity demand.

2. Case Study: Hospital

In order to demonstrate the use and results of a computational algorithm for the evaluation of internal combustion engine cogeneration systems, the typical loads of a hospital were chosen as a case study. By examining electricity and gas bills, and inspecting the installed equipment (chillers, boilers, water heaters, etc.), profiles for the hospital energy demands were constructed. Currently, the hospital purchases electricity from the grid. It produces hot water in a boiler, and steam in a steam generator, both fueled by LPG (liquefied petroleum gas).

Figure 1 shows a typical electric demand profile. The figure was constructed with consumption data at peak and out-of-peak hours throughout the year of 2003. *Figure 2* shows a typical demand profile of hot water for sanitary purposes (50°C), and saturated steam demand at 7 bar (700 kPa). This estimate was based on the equipment technical data and on the gas bill. *Figure 3* shows the cooling load (air

conditioning) profile, based on equipment characteristics, hospital activity, and typical cooling load profiles for the summer in the region. *Figure 4* presents a typical summer weather profile. Summer loads were assumed for the simulation. *Figure 5* represents the cogeneration configuration assessed here; flows are identified in the text by brackets.

3. Methodology

The results presented here were obtained through software consisting of FORTRAN engineering programs and a Delphi interface. Graphical results are directly generated by a spreadsheet file (Excel) that imports data from result files. The FORTRAN program is composed of one main algorithm and more than 20 subroutines, including i) five different engines, ii) water and steam properties, iii) exhaust gas properties, iv) absorption chiller selection, v) absorption chiller simulation, vi) heat recovery steam generator (HRSG) simulation, vii) pre-heater design, viii) pre-heater simulation, ix) exhaust gas heat exchanger design, x) exhaust gas heat exchanger simulation, among others.

The main program controls data entry, results and all calculation procedures. Calculation procedures use curve fitting of polynomial expressions (engine and absorption chiller performance); deterministic modeling or mathematical representations of physical phenomena (heat transfer and pressure drops); and physical properties (water and exhaust gases). A computational algorithm involving several iterative procedures was developed, constituting an integrated thermal system that considers all equipment as operating as a single system. It produces results as a function of demands, energy supplied by engine, design parameters, etc. A thermal system integration overview can be seen in Smith (2005).

The hourly profile analysis simulation applied here approximates the dynamic nature of energy consumption in buildings and the dynamics of thermal equipment performance in an integrated system by a series of quasi-steady-state operating conditions with one-hour time-steps, as used by Lebrun (1999).

Some computational routines developed in previous papers were used in this project, including: gas turbines cogeneration (Espirito Santo and Gallo, 1999 and 2000), combined cycle (Espirito Santo and Gallo, 2001), and combined cycle optimization (Espirito Santo 2003). Other simulations of internal combustion engine cogeneration system configurations developed with this software can be seen in Espirito Santo 2005, 2006.

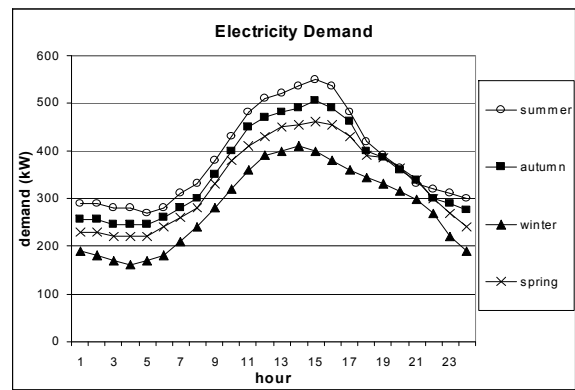


Figure 1. Electricity demand (kW).

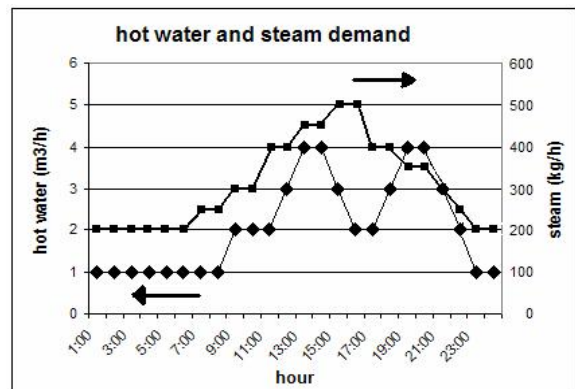


Figure 2. Hot water (m³/h) and steam demand (kg/h).

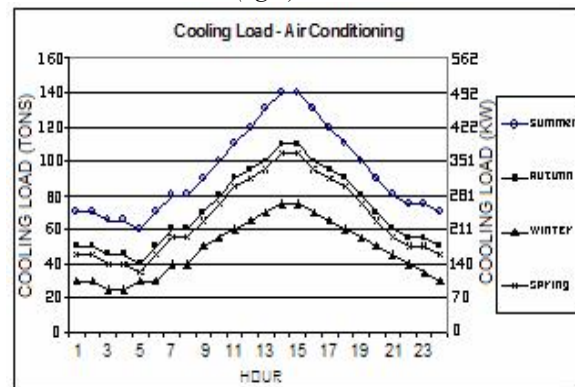


Figure 3. Cooling load (tons and kW).

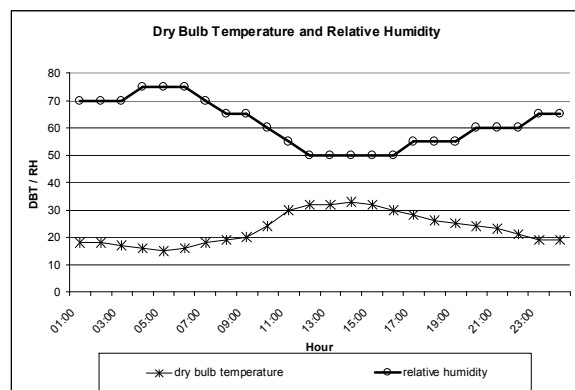


Figure 4. Local weather profile (summer).

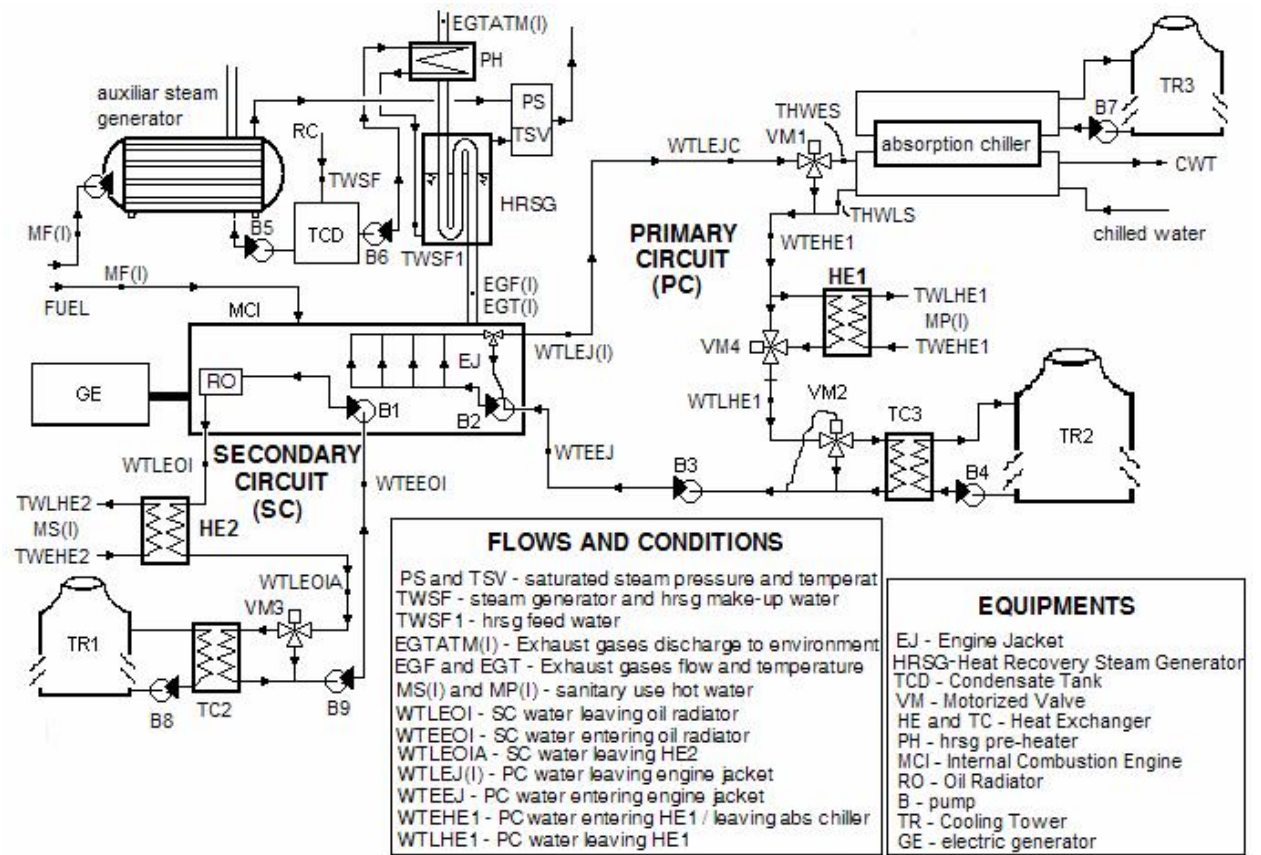


Figure 5. Cogeneration scheme.

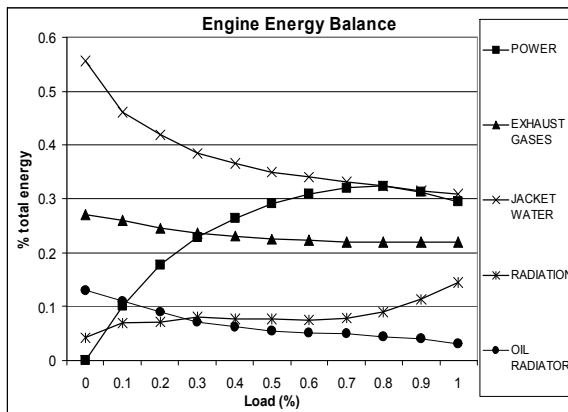


Figure 6. Engine A - energy balance.

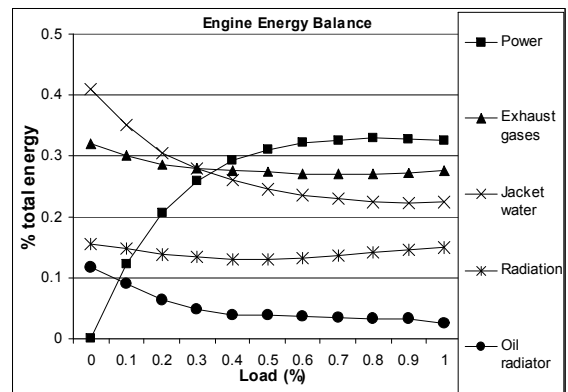


Figure 8. Engine B - energy balance.

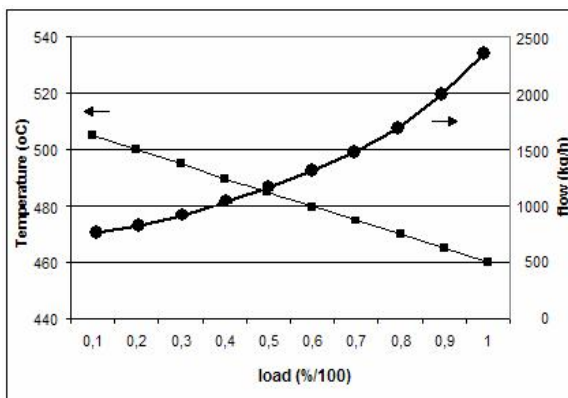


Figure 7. Exhaust gas flow and temperature (engine A).

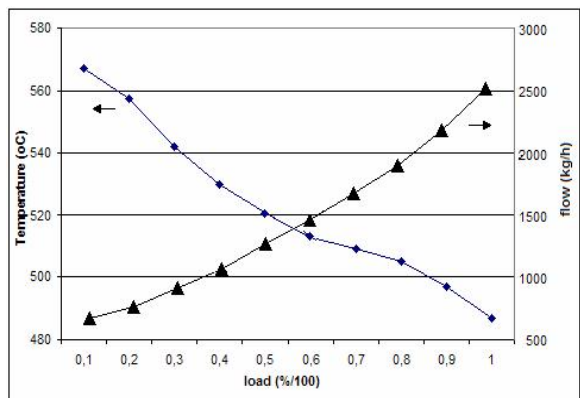


Figure 9. Exhaust gas flow and temperature (engine B).

4. Cogeneration Configuration

The cogeneration system in *Figure 5* is constituted by one internal combustion engine, primary and secondary hot water circuits, one heat recovery steam generator (HRSG), one HRSG pre-heater, one water-LiBr hot water absorption chiller, and auxiliary equipment (pumps, cooling towers, heat exchangers, etc.). The secondary circuit recovers energy from the engine oil radiator and uses it to warm water for sanitary purposes. The primary circuit recovers energy from the engine jacket and uses it in an absorption chiller, as well as to warm water for sanitary purposes (after recovery in the secondary circuit). Energy from the exhaust gases is used for steam generation in an HRSG with pre-heater.

Figure 6 shows the energy balance of engine A, and *Figure 7* the exhaust gas flow and temperature as a function of engine load. Maximum engine efficiency is found at a load near 0.8 (32.3%), and thermal efficiency at full load is 29.5%. Primary circuit hot water is designed to enter engine A at 89°C [WTEEJ] and leave it at 99°C [WTLEJ(I)].

Figure 8 represents the energy balance of engine B, and *Figure 9* the exhaust gas flow and temperature as a function of engine load. Maximum engine efficiency is also found at a load near 0.8 (33%), and thermal efficiency at full load is 32.5%. Primary circuit hot water is designed to enter engine B at 85°C [WTEEJ] and leave it at 95°C [WTLEJ(I)].

Energy balances of engines A and B were obtained from ASHRAE (2000). Engine A is naturally aspirated, and Engine B turbocharged. Exhaust gas flow and temperature curves are based on information from an engine manufacturer, and are compatible with the energy in exhaust gases. Design temperatures of hot water at the primary and secondary circuits are based on typical values. Correction for atmospheric pressure (not applicable in this study) considers a 0.7% loss of power for each additional 100 meters above 500 meters. Correction for dry bulb temperature considers a 0.5% loss of power for each degree Celsius above 25°C.

In this study, engines A and B have both an output power of 425 kWe, and they are compared as prime movers in the cogeneration configuration shown in *Figure 5*.

5. Design Parameters

The systems operate in electrical dispatch, i.e., the engine net electric power follows electric demand.

Primary circuit energy is recovered at a hot water absorption chiller. After leaving the absorption chiller [WTEHE1], hot water can pass

through HE1 (heat exchanger to warm sanitary use water) if the water temperature leaving the absorption chiller is higher than the design temperature at the engine entrance (89°C for engine A and 85°C for engine B). The single-effect absorption chiller has a nominal capacity of 520.4 kW (148 tons) for the engine A scheme, and 393.8 kW (112 tons) for the engine B scheme. The capacity is based on saturated steam at 82.5 kPa as the heat source, chiller water being produced at 7.2°C (5.5°C of temperature difference) and water entering the condenser at 29.4°C. Absorption chiller simulation is based on curves for equipment selection and performance from an absorption chiller manufacturer (Trane Company, 1989), considering that the chilled water temperature leaving the absorption chiller is 7.2°C (5.5°C temperature difference), condensing water enters at 29.4°C (fixed), assuming that the flow at condenser and absorber is as required by the manufacturer. These data represent the design condition of the existing chilled water plant at the hospital. More about energy recovery and standard tests in absorption chillers can be found in ARI (1992) and Dorgan (1995).

The heat recovery steam generator and pre-heater were designed according to the methodology proposed and used by Ganapathy (1991). Saturated steam is produced at 7 bar (165°C). The HRSG physical characteristics are: 100 tubes (engine A scheme) and 120 tubes (engine B scheme), both with a diameter of 25.4 / 37.8 mm (internal/external) and a length of 4.0 meters. Heat loss of 2% and blowdown of 2% were also assumed. Exhaust gas composition is regarded as constant, and properties are evaluated at mean temperature in the HRSG and HRSG pre-heater. Make-up water [TWSF] enters the condensate tank at 70°C (fixed) and HRSG feed water [TWSF1] leaving the pre-heater was designed to achieve a 10°C approach point. A heat loss of 2% was assumed for the HRSG pre-heater.

Under design conditions the secondary circuit hot water enters [WTEEOI] both engines at 35°C (fixed) and leaves [WTLEOI] at 50°C. Water flows at the primary and secondary circuit are designed considering the energy at the circuit and the design temperature difference (constant flow).

Heat exchangers HE1 and HE2, used to recover energy from the primary and secondary circuits (hot water for sanitary purposes), were designed to achieve approach points of 5.6°C and 1.7°C respectively. Sanitary use hot water recovers energy at HE2 and HE1 in a series arrangement [MS(I) = MP(I)].

Cooling towers and auxiliary heat exchangers are required to reject unused energy, preventing engines from operating in unsafe

conditions. Design of this equipment was not undertaken.

The total electricity produced is 3% higher than net engine power, taking into account the use of electricity in auxiliary equipment (parasitic load). The absorption chiller replaces electrical consumption of air cooled reciprocating compressor chillers. A fixed rate of 1.0 kW/ton was assumed. No heat loss at pipes and ducts was considered.

6. Technical Results

6.1 Electricity

Figure 10 shows the electricity balance obtained by simulation of engines A and B. Due to the replacement of part of the cooling load from reciprocating compressor chillers by the absorption chiller, two new electricity demands can be predicted, one for each engine under analysis. Engine A operates at part load from hours 1 to 11 and 17 to 24; from hours 12 to 16 it operates at full load, and complementary electricity must be bought from the grid. The absorption chiller used with engine A replaces electrical demands between 45 kW (hour 4) and 85.6 kW (hour 16).

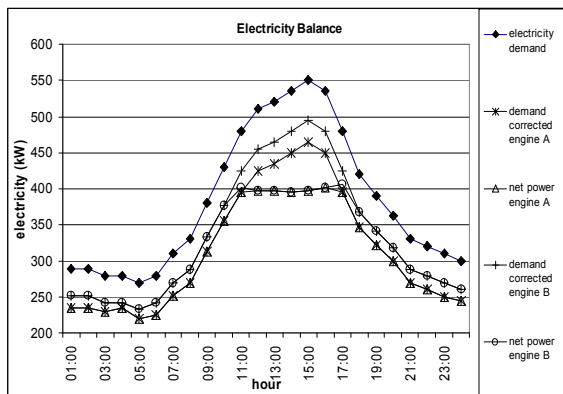


Figure 10. Electricity balance (engines A and B).

Analysis of engine B reveals that the avoided electrical demand at the absorption chillers varies between 36.2 kW (hour 5) and 55.7 kW (hour 17). A corrected electricity demand curve can also be predicted (Figure 10). Engine B operates at full load between hours 11 to 17, and complementary electricity must be bought from the grid. The engine A scheme replaces more electricity (avoided at the absorption chiller), and as a consequence has a lower load factor.

6.2 Absorption chiller

Figure 11 shows the cooling load and the absorption chiller capacity obtained in the simulation with engine A and engine B schemes. Figure 12 depicts the primary circuit hot water temperature at the absorption chillers. In the engine A scheme, at hours 1 to 6 and 23 to 24 the

absorption chiller operates at part load (hot water by-pass occurs matching cooling load); as a result, primary circuit water enters the chiller at about 95°C [WTLEJ(I)] (engine load function) and leaves it just above 89°C [WTEHE1] (mixture temperature). At hours 7 to 10 and 18 to 22 the energy supplied by the engine at the primary circuit and the absorption chiller generator heat transfer capability changes the matched equilibrium operation point. (By "matched equilibrium operation point" we mean the steady state operation condition that results from the performance characteristics of the various pieces of equipment.) At hour 7, for example, engine load is 0.61, and the primary circuit water leaves the engine to enter the absorption chiller at 87.4°C, and leaves the absorption chiller at 81°C. At hours 11 to 17, the absorption chiller produces 298.9 kW (85 tons), and the primary circuit water temperature is near the design condition. The hot water temperature difference at the absorption chiller varies from 4.3 to 9.3°C.

For the engine B scheme, Figure 11 shows that the absorption chiller always operates at full load. The matched operation between the engine disposable energy and the absorption chiller heat transfer changes primary circuit design condition at hours 1 to 9 and 18 to 24 (Figure 12). The hot water temperature difference at engine B varies between 6.1°C and 9.2°C.

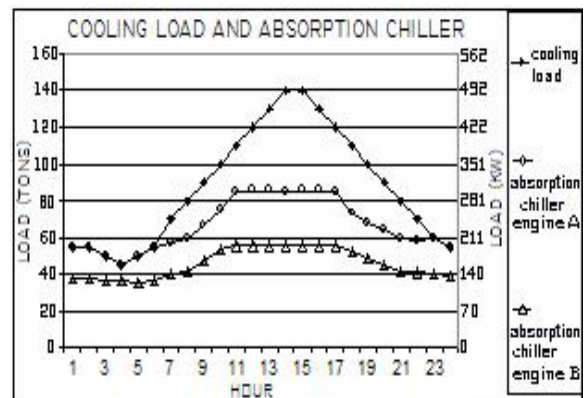


Figure 11. Cooling load (engines A and B).

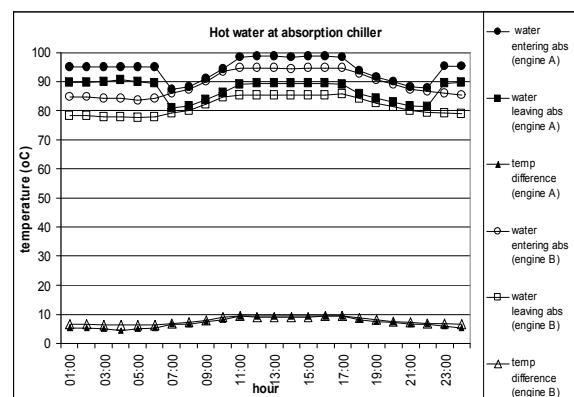


Figure 12. Hot water at absorption chiller (A and B).

The absorption chiller coefficient of performance (COP) at full load is between 0.71 and 0.72. The engine A scheme has a slightly higher COP due to a higher water temperature. When the absorption chiller in the engine A scheme operates at part load, a higher COP is achieved. At hour 4 a COP of 0.82 is calculated (figure not shown).

6.3 Steam Generation

Steam generation profiles obtained for engine A and B schemes can be seen in *Figure 13*. A rise in steam generation occurs when the engine operates at a higher load factor, due to the higher exhaust gas flow, in spite of a reduction on exhaust gas temperature (*Figures 7 and 9*).

Analysis of engine A reveals that between hours 1 and 6 steam generation approaches demand, but does not quite meet it. Additional steam must be produced from hours 1 to 22. At hours 23 and 24 a by-pass of part of the exhaust gases occurs (figure not shown). Analysis of engine B reveals that between hours 1 and 10 as well as between 22 and 24, a by-pass of part of the exhaust gases must be done to adjust steam generation to demand. At hours 11 to 21 additional steam must be produced in a complementary steam generator.

Figures 14 and 15 represent the exhaust gases temperature leaving the engines and passing through the HRSG and the HRSG pre-heater. Exhaust gases that by-passed the HRSG are subsequently mixed to gases that effectively passed through it. *Figure 14*, representing the engine A scheme, shows that a small by-pass factor (about 2%) at hours 23 and 24 does not significantly change the discharge temperature. For engine B (*Figure 15*), the temperature of gases discharged to the atmosphere [EGTATM(I)] (gas mixture temperature) is higher as a result of higher by-pass factors.

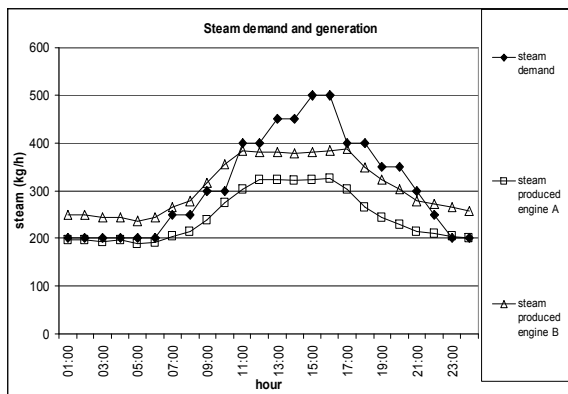


Figure 13. Steam demand and generation (engines A and B).

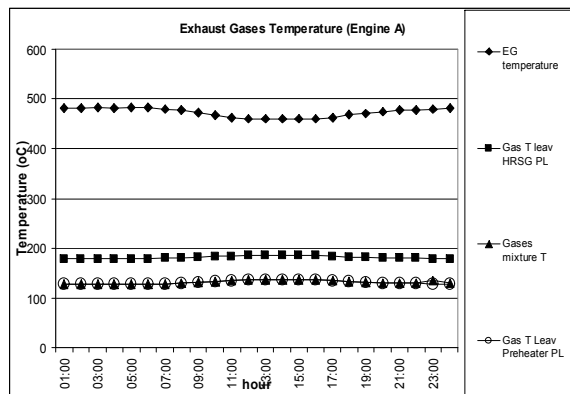


Figure 14. Exhaust gas temperature (engine A).

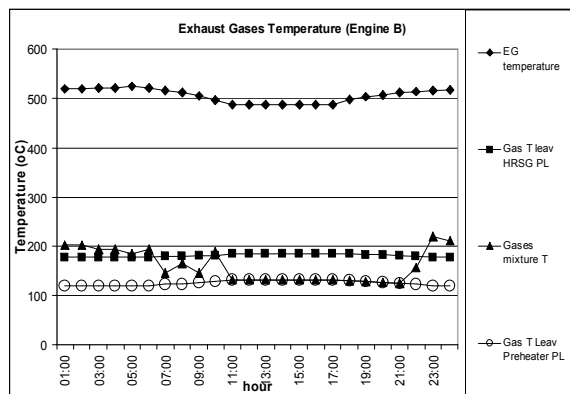


Figure 15. Exhaust gas temperature (engine B).

As shown in *Figure 16*, during the hours when the engines operate at full load, the HRSG feed water temperature [TWSF1] is 155.5°C, confirming the design condition of the HRSG pre-heater (10°C of approach, since the saturated steam temperature at 7 bar (700 kPa) is 165°C). Temperatures of HRSG feed water are lower when engines operate at part load, and exhaust gas by-pass occurs.

6.4 Engine secondary circuit (SC)

Energy from the secondary circuit is recovered to warm water for sanitary purposes [MS(I)]. Sanitary water enters HE2 (heat exchanger 2, *Figure 5*) at 22.2°C (fixed). In the engine A scheme (*Figure 17*), secondary circuit water leaves the engine [WTLEOI] at 49°C at hours 1 through 6, and 23 through 24. At hours 10, 11, 17 and 18 it reaches 51°C, as a result of a quick rise in the oil radiator participation in the engine energy balance between loads 1 and 0.9. Sanitary use hot water leaves HE2 between 32 and 48°C, depending on three factors: demand (*Figure 3*), energy provided by the engine, and the design heat exchanger approach point. From hours 1 to 8, and 23 and 24 energy is being rejected at the cooling tower (TR1) (the secondary circuit hot water leaving HE2 [WTLEOIA] is close to 39°C), but the heat exchanger (HE2) approach point is met. A similar situation can be seen in *Figure 18* for the engine B scheme. Recoverable energy in

the secondary circuit ranges from 28 to 50 kWh and from 28 to 36 kWh for engines A and B, respectively. Unrecovered energy is rejected at TC2 and TR1 (Figure 5).

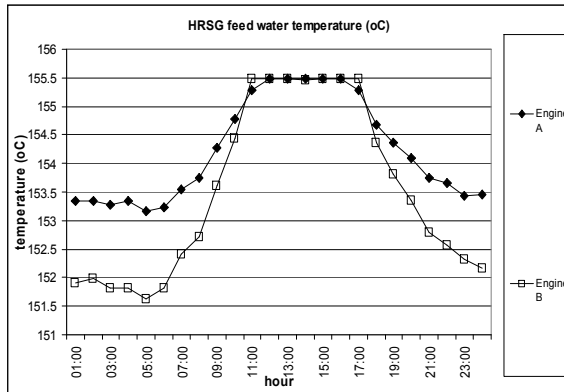


Figure 16. HRSG feed water temperature.

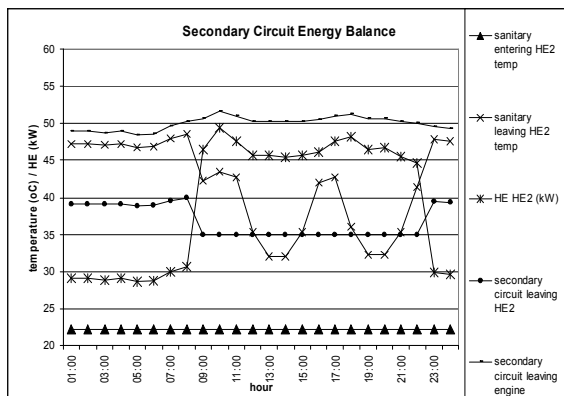


Figure 17. Secondary circuit balance (engine A).

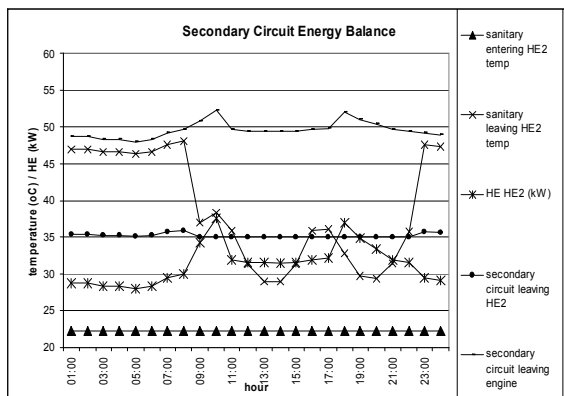


Figure 18. Secondary circuit balance (engine B).

6.5 Engine primary circuit (PC)

Sanitary water enters HE1 at the same temperature as it leaves HE2 (Figures 17 and 18).

The engine A primary circuit energy balance can be seen in Figure 19. Energy recovery to warm hot water for sanitary purposes occurs only during hours when energy is available: 1 to 6, 11 to 17, and 23 to 24, because the temperature of primary circuit water returning to the engine [WTEHE1] is higher than the design condition (89°C). If the primary circuit hot water leaves the

absorption chiller below 89°C (primary circuit hot water design condition), then it by-passes HE1, and no energy is recovered. In order to maintain a fixed design condition, an auxiliary boiler must warm the sanitary use hot water to the design condition (50°C).

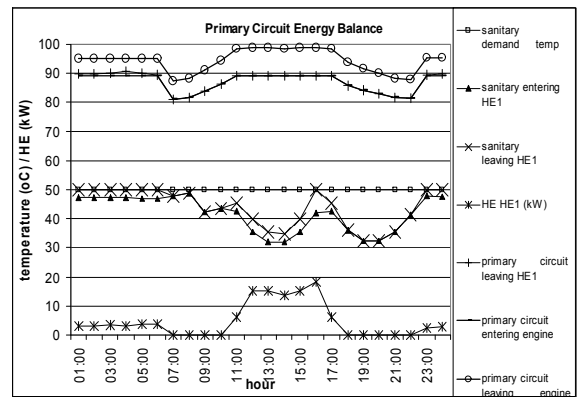


Figure 19. Primary circuit balance (engine A).

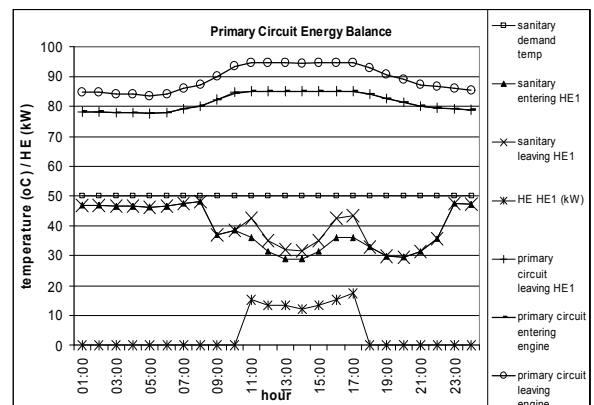


Figure 20. Primary circuit balance (engine B).

Figure 20 presents the results obtained with the engine B scheme. Energy is available only at hours 11 to 17, as a consequence of two factors: (1) full load engine operation and, (2) the fact that the primary circuit hot water temperature difference at the absorption chiller [WTLEJ(I)-WTEHE1] is somewhat lower than the design condition [WTLEJ(I)-WTEEJ]. Both the heat exchanger TC3 and the cooling tower TR2 reject unrecovered energy from the primary circuit.

6.6 Energy utilization factor (EUF)

In the present work, the energy utilization factor is defined as the percentage of energy recovered from the engine fuel to meet a particular energy demand.

The individual engine A EUF analysis reveals an engine electric participation between 28.9 and 31.1%, with the higher values occurring at an engine load near 0.8. Absorption chiller participation varies from 25 to 34%. Exhaust gas energy utilized for steam generation has a participation of about 14% at the HRSG, and about 2.4% at the HRSG pre-heater. HE2 has a 4

to 5% contribution, and HE1 reaches 1.3% at hour 16 (Figure 21). Figure 22 presents the EUF achieved with the engine B scheme. Engine electric efficiency approaches 31%. The participation of absorption chiller EUF ranges from 21.1 to 23.8%. Exhaust gas for steam generation ranges from 13.7 to 18% at the HRSG, and from 2.4 to 3.9% at the HRSG pre-heater. HE2 ranges from 2.5 to 3.7%, and HE1 from 0.9 to 1.3%. Engine electric participation in Figures 21 and 22 was computed after deducting electricity for auxiliary equipment (parasitic loads).

The final EUF (Figure 23) is the sum of individual fractions shown in Figures 21 and 22. A higher mean value was achieved for the engine A scheme: 81.4% versus 76.7% for engine B. Some of the reasons contributing to the higher EUF of engine A are: (i) a lower participation of radiation (heat loss from the engine to the environment) at part load (Figures 6 and 8); (ii) an exhaust gas by-pass equal to zero at hours 1 to 22 (Figure 14); (iii) a higher than nominal thermal efficiency at engine A loads between 0.55 and 0.95; and (iv) a better match of the hospital electrical and thermal loads.

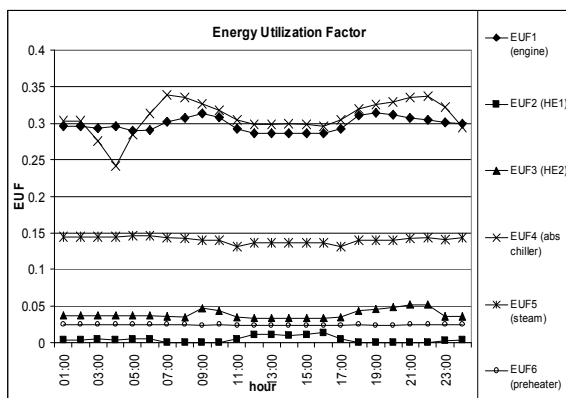


Figure 21. Energy utilization factor (engine A).

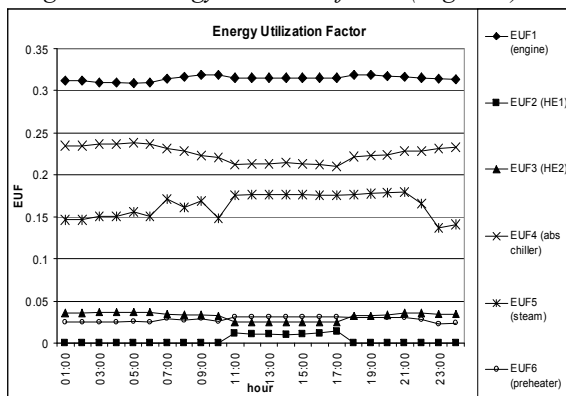


Figure 22. Energy utilization factor (engine B).

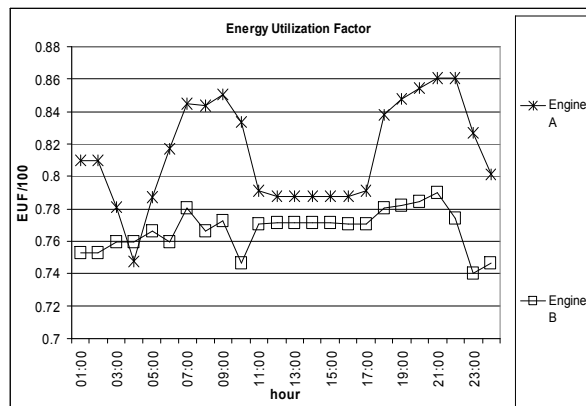


Fig. 23 - Final energy utilization factor

7. Conclusions

The engine A scheme was found to be more flexible for higher demands of electricity and chilled water, since the engine load factor is lower than that of engine B, and the absorption chiller has a higher real capacity. On the other hand, higher steam demand favors the engine B scheme, because part of the exhaust gases is by-passed.

One might expect that a higher EUF cogeneration system could be built around engine B, since thermal efficiency of engine A is 29.5% and engine B is 32.5%. However, the engine energy balance under partial loads, the electrical dispatch operation mode, and a better match of thermal loads conferred to engine A a higher final EUF.

TABLE I presents a daily kWh energy analysis for the hospital. Consumption of electricity, hot water and steam is 15907.6 kWh per day (column 1 of TABLE I), disregarding conversion factors (efficiency). Assuming an efficiency of 30% for electricity production and 80% for steam and hot water production, the energy daily consumption rises to 39015.75 kWh (second column of TABLE I). From TABLE I, the cogeneration system with engine A is expected to consume 24712.1 kWh/day of natural gas (column 4), and with engine B 24298.4 kWh/day (column 6), producing 7567.93 kWh and 7888.11 kWh of electricity and importing from the grid 232.43 kWh and 423.27 kWh of electricity respectively (columns 3 and 5). The cogeneration scheme with engine A would require an additional 554.99 kWh to warm sanitary use hot water to the design condition, whereas with engine B 763.82 kWh would be used. In order to meet steam demand, the engine A scheme needs 1080.1 kWh/day, and the engine B scheme needs 393.9 kWh/day (columns 3 and 5 of TABLE I).

Columns 4 and 6 show the final results, based on the conversion factors given above. The engine B scheme is expected to consume 1.4% less energy than the engine A scheme. Comparing the actual demand of energy (39015.75 kWh) and

the energy demand with engine A (27530.7 kWh) and engine B (27156.42 kWh) cogeneration systems, reductions of primary energy consumption of 29.4% and 30.4% were obtained, respectively.

A higher primary circuit hot water temperature favored engine A in this comparison, since more capacity is obtained at the absorption chiller and more electricity is avoided at electrical chillers. A higher electrical substitution factor for the absorption chiller replacing the electrical chillers can make the engine A scheme consume less energy. The central chilled water plant should use the absorption chiller whenever possible, and utilize air cooled reciprocating chillers only when necessary to cover the cooling load.

The final decision should take into account initial investment, maintenance support and costs, electrical and thermal load variations throughout the year, electricity contract rules, taxes,

operational costs, and others factors cited by Hu (1985) and Orlando (1996).

Different decision criteria can lead to different engine choices. Taking the EUF as the decision criterion, engine A should be chosen, whereas primary energy savings would point to engine B as the more attractive one. Primary energy savings depend on the mean thermal efficiency of the existing thermal plants, the steam and hot water production efficiencies, and the quantity and type of energy demands replaced by the cogeneration system.

The use of a computational algorithm to evaluate some influences of engine characteristics on cogeneration system design was presented. Economic and second law analysis will be developed in future studies.

TABLE 1 - DAILY ENERGY ANALYSIS (kWh)

	actual		engine A		engine B	
	consumption (kWh)	consumption (kWh)	complementary consumption (kWh)	complementary consumption (kWh)	complementary consumption (kWh)	complementary consumption (kWh)
	no conversion	with conversion	no conversion	with conversion	no conversion	with conversion
1 electricity consumption (kWh)	9183,00	30610,00	232,43	774,77	423,27	1410,90
2 hot water consumption (kWh)	1615,30	2019,13	554,99	693,74	763,82	954,78
3 steam consumption (kWh)	5109,30	6386,63	1080,11	1350,14	393,90	492,38
4 cogeneration natural gas (kWh)	-	-	-	24712,06	-	24298,37
5 total energy	15907,60	39015,75	-	27530,70	-	27156,42

References

ARI - Air Conditioning & Refrigeration Institute, 1992, Standard 560-92: Standard for absorption water chilling and water heating packages. N. York.

ASHRAE ,2000, *Systems and Equipment Handbook* (Chapter 07).

Dorgan, C. B., Leight, S. P., Dorgan, C. E., 1995, *Application Guide for Absorption Cooling / Refrigeration Using Recovered Heat*. ASHRAE Publication. Atlanta.

Espirito Santo, D. B. and Gallo W. L., 1999, "Energetic and Economic Analysis of a Gas Turbine Cogeneration System for a Hospital". *Ecos '99*, Tokyo, Japan.

Espirito Santo, D. B. and Gallo W. L., 2000, "Predicting Performance of a Gas Turbine Cogeneration System with Inlet Air Cooling". *Ecos '2000*, Twente, Netherlands.

Espirito Santo, D. B. and Gallo W. L., 2001, "Evaluating a Dual Pressure Combined Cycle Power Plant". *Ecos '2001*, Istanbul, Turkey.

Espirito Santo, D. B., 2003, "Exergetic and Energetic Evaluation of a Triple Pressure Heat Recovery Steam Generator with Reheat", *Ecos '2003*, Copenhagen, Denmark.

Espirito Santo, D. B., 2005, "Simulation of Internal Combustion Engines Cogeneration Systems: Four Different Engines Sizes with Hot Water Absorption Chiller". *Ecos '2005*, Trondheim, Norway.

Espirito Santo, D. B., 2006, "Evaluating an Electricity Base Load Engine Cogeneration System – Electricity, Steam and Hot Water – Through a Computational Simulation Methodology". *Ecos '2006*, Crete, Greece.

Ganapathy, V., 1991, *Waste Heat Boiler Deskbook*. Fairmont Press, Lilburn.

Hu, SD., 1985, *Cogeneration*. Reston Publishing House, Reston:.

Lebrun, Jean, Bourdouxhe Jean-Pascal and Grodent Marc, 1999, 'A Toolkit for Primary HVAC System Energy Calculation – *ASHRAE 1999*'. Laboratoire de Thermodynamique, Université di Liège.

Orlando, J. A., 1996, *Cogeneration Design Guide*. Ashrae.

Smith, R., 2005, "Process Integration: Current Status and Future Potential", *Ecos '2005*, Norway.

The Trane Company, 1989 "Single Stage Absorption Cold Generator 101 to 1660 Tons".